First Principles Treatment of Configuration Optimizations, Excited-State Properties, and Dynamic Third-Order Polarizabilities of Chloro-Metal Phthalocyanines MPcCl (M = Al, Ga, In)

D.-S. Wu, W.-D. Cheng,* X.-D. Li, Y.-Z. Lan, D.-G. Chen, Y.-C. Zhang, H. Zhang, and Y.-J. Gong

Fujian Institute of Research on the Structure of Matter, Chinese Academy of Sciences, Laboratory of Materials Chemistry and Physics, Fuzhou, Fujian 350002, People's Republic of China

Received: August 24, 2003; In Final Form: January 14, 2004

We report optimized geometrical structures at the RHF/6-31G* and 3-21G levels, the properties of excited states using time-dependent density functional theory based on the B3LYP/3-21G* level, and the frequency dependence of third-order nonlinear optical polarizabilities γ in different optical processes of THG, EFISHG, and DFWM by using B3LYP coupled with the sum over states methods (SOS//TDDFT-B3LYP/3-21G*) for the MPcCl (M = Al, Ga, In) molecules. The calculated results show that both the distance of the central atom from the Pc plane and the γ value increase in the order of AlPcCl < GaPcCl < InPcCl. The dispersion behaviors of the three different optical processes are discussed, and the calculated susceptibilities of $\chi^{(3)}(-\omega; \omega, \omega, -\omega)$ match the measured values and correspond to the varied trends in the measurements of AlPcCl < GaPcCl < InPcCl films. It is found that a large ionic radius of M makes a large distortion away from C_{4v} symmetry and that a larger d-electron transfer results in a red shift in the absorption spectrum and a large third-order nonlinear optical susceptibility among the MPcCl (M = Al, Ga, In) materials.

1. Introduction

Phthalocyanines (Pcs) and their derivatives exhibit peculiar and unconventional physical properties[1] and have become important materials for applications in photovoltaics, electrochromism, optical data storage, laser dyes, liquid crystals, chemical sensors, and photosensitizers for photodynamic therapy[2,3] as well as catalysts for the aziridination of olefins.[4] They are currently of great scientific and technological interest for designing novel electronic and photonic devices because of their properties as semiconductors as well as their large linear and nonlinear optical responses. The bulk third-order susceptibility measured in thin films and crystals and the isotropically averaged molecular third-order polarizability measured in solution have been obtained for a variety of free-base and metallo-substituted Pc compounds.[5−12] AlPc as a nonlinear chromophore is incorporated into the polymer system, and this system has a large third-order nonlinear optical response.[13] Third-order nonlinearities are of special interest because they provide a mechanism for all-optical devices. Furthermore, the realization of all-optical switching, modulating, and computing devices is an important goal in modern optical technology. Nonlinear optical materials with large third-order nonlinear susceptibilities are indispensable for such devices because the magnitude of this quantity dominates the device performance. It has been known that material structures strongly influence device performance for a long time; the exact relationship between the structures of Pc complexes and their device performances, however, still remains unclear. A part of this mystery is certainly due to the lack of comprehensive investigations of electronic and space structures.

Generally, Pc complexes are centrosymmetric planar organic molecules with 2D conjugated π-electron delocalization. The 2D π-conjugated system in Pc allows for the tailoring of chemical and physical properties over a very wide range of chemical modifications by incorporating many different metal atoms into the ring and by substituting various functional groups at peripheral sites. The common feature of Pc complexes is a basic structure consisting of four pyrrole units that are linked in a circular manner by azamethine bridges. The hole in the center of Pc complexes can accommodate metals, semi-metals, or hydrogens, where the central atom coordinates with the pyrrole nitrogens (N_{py}). The role of the centered metal atom of PcM in the nonlinear optical (NLO) response is a problem of physical relevance, and it has been addressed in a number of studies using both solutions and thin films.[14−16] The possibility of introducing different centered metal atoms provides architectural flexibility to optimize the NLO and other physical properties. However, no significant differences with different centered metal atoms have been observed for $|\gamma(-3\omega; \omega, \omega, \omega)|$ values ranging from 2.45×10^{-32} to 4.57×10^{-32} esu in R_8PcM (M = H_2, Cu, Ni, Co) at an input wavelength of 1.340 μm[14] and for $\chi(-3\omega; \omega, \omega, \omega)$ values ranging from 0.60×10^{-12} to 0.76×10^{-12} esu in PcM (M = Co, Ni, Pt).[17] Experimental evidence of which the $\chi(-3\omega; \omega, \omega, \omega)$ values of PcM containing axial substitutes are larger than those having no axial substitutes has been obtained.[18] The MPcCl compounds have the same axial substituent atom Cl and a different centered atom M. The third-order nonlinear optical susceptibilities $\chi(-3\omega; \omega, \omega, \omega)$ of these MPcCl (M = Al, Ga, In) films were determined to be 1.5×10^{-11} esu (input wavelength 1907 nm), 2.5×10^{-11} esu (input wavelength 1064 nm), and 13.0×10^{-11} esu (input wavelength 1907 nm), individually.[9,17] Accordingly,

* Corresponding author. E-mail: cwd@ms.fjirsm.ac.cn.

10.1021/jp0365211 CCC: $27.50
Published on Web 02/13/2004

we can understand the origin of this excessively large susceptibility in InPcCl films.

Additionally, metal phthalocyanines (PcM) are very stable organometallic materials undergoing no noticeable degradation in air up to 400−500 °C. Although this exceptional thermal stability together with large chemical versatility makes it feasible to obtain single crystals of a number of phthalocyanines by successive sublimation, the single-crystal structure of the InPcCl compound has not yet been reported. Recently, Hanack and coworkers reviewed the synthesis of different peripheral and axially substituted indium phthalocyanines and described how the resulting changes in the steric and electronic properties alter their linear and nonlinear optical properties.[19] To make systematic comparisons, in this study we optimize the geometrical structures and calculate the excited-state properties and third-order polarizability spectrum of the three MPcCl (M = Al, Ga, In) compounds using the first principles method. We also examine the structural and compositional contributions to the third-order nonlinear optical properties.

2. Computational Procedures

Geometrical optimizations at the RHF/6-31G* and 3-21G levels are carried out using the program Gaussian 98.[20] The degrees of freedom are 168, and the maximum allowed number of steps is 348 during the stepwise search for local minima on energy surfaces of three MPcCl molecules in the geometry optimizations. A convergent value of the rms density matrix is the default in Gaussian 98, and a local minimum is searched in view of the updated second derivatives for MPcCl (M = Al, Ga, In), individually. After the convergent values (set by default in Gaussian 98) of the maximum force, rms force, maximum displacement, and rms displacement are reached, the zero of the first derivatives and the positives of the second derivatives are obtained on a potential energy surface for MPcCl molecules. A zero length of all gradient vectors (first derivatives) characterizes a stationary point, and a minimum corresponds to a point having positive second derivatives. Equivalently, all of the forces on the atoms in a molecule are zero, and the force constant is positive. In classical mechanics, the first derivative of the potential energy of a particle is the negative of the force on the particle, and the second derivative is the force constant. Accordingly, a minimum stationary point on the energy surfaces corresponds to the equilibrium geometry of an MPcCl molecule.

The properties of excited states are computed by using time-dependent density functional theory (TDDFT) at the B3LYP/3-21G* level[21−23] after MPcCl (M = Al, Ga, In) molecular geometries are obtained. The calculations are performed with Gaussian 98.[20] Becke's three-parameter Lee−Yang−Parr (B3LYP) hybrid function including exact exchange and the correlation function along with the standard basis sets of 3-21G* stored internally in the Gaussian 98 program[20] are employed in the calculations. The wave functions and energy eigenvalues of the excited states are determined by solving the time-dependent Kohn−Sham equation.[24,25] The SCF convergence criteria of the rms density matrix and the maximum density matrix are set at 10^{-8} and 10^{-6}, respectively, in all of the electronic structure calculations. The range of molecular orbitals for correlation is from orbital 51 to orbital 430, orbital 55 to orbital 440, and orbital 64 to orbital 550, individually for MPcCl (M = Al, Ga, In), and the core orbitals are frozen in the TDDFT calculations. The iterations of excited states are continued until the changes in the state energies are no more than 10^{-7} au between the iterations and convergence has been obtained in the all calculations.

In the nonresonant region, the third-order polarizability tensor γ of MPcCl can be described by the conventional sum-over-states (SOS) expression:[26,27]

$$\gamma_{abcd}(-\omega_p;\omega_1,\omega_2,\omega_3) = \left(\frac{2\pi}{h}\right)^3 K(-\omega_p;\omega_1,\omega_2,\omega_3)e^4 \left\{\sum_P\left[\sum_{i,j,k}{}'\left(\frac{\langle o|r_a|k\rangle\langle k|r_b{}^*|j\rangle\langle j|r_c{}^*|i\rangle\langle i|r_d|o\rangle}{(\omega_{ko}-\omega_p)(\omega_{jo}-\omega_1-\omega_2)(\omega_{io}-\omega_1)}\right)\right] - \sum_P\left[\sum_{j,k}{}'\left(\frac{\langle o|r_a|j\rangle\langle j|r_b|o\rangle\langle o|r_c|k\rangle\langle k|r_d|o\rangle}{(\omega_{jo}-\omega_p)(\omega_{jo}-\omega_1)(\omega_{ko}+\omega_2)}\right)\right]\right\} \quad (1)$$

Hereafter, the symbols $\gamma(3\omega)$, $\gamma(2\omega)$, and $\gamma(\omega)$ represent the third-order polarizability of the third-harmonic generation (THG) of $\gamma(-3\omega;\omega,\omega,\omega)$, the electric-field-induced second-harmonic generation (EFISHG) of $\gamma(-2\omega;\omega,\omega,0)$, and degenerate four-wave mixing (DFWM) of $\gamma(-\omega;\omega,\omega,-\omega)$, individually. The prefactor $K(-\omega_p;\omega_1,\omega_2,\omega_3)$ must be taken as the same value for THG, EFISHG, and DFWM in the static case of an input photon energy of zero, and it is the relative magnitudes of the ground-state nonlinear polarizabilities for each optical process at nonzero frequency.[28] In the following calculations, we use the same prefactor K in order to make the remark to justify plotting curves for the three types of nonlinear polarizability against common axes. In eq 1, $\langle o|r_a|k\rangle$ is an electronic transition moment along the a axis of the Cartesian system between the reference state (ground state) $\langle o$ and excited state $\langle k$; $\langle k|r_b{}^*|j\rangle$ denotes the dipole difference operator equal to $[\langle k|r_b|j\rangle - \langle o|r_b|o\rangle\delta_{kj}]$; $\hbar\omega_{ko}$ is the energy difference between state k and reference state o; ω_1, ω_2, and ω_3 are the frequencies of the perturbating radiation fields; $\omega_p = \omega_1 + \omega_2 + \omega_3$ is the polarization response frequency; Σ_P indicates a summation over the 24 terms obtained by permuting the frequencies; Σ' indicates a summation of $i, j, k \neq o$. Here, it is noted that the γ component is expressed mathematically in terms of transition moments between excited electronic states and the energies of these excited states in eq 1; furthermore, the state energy depends on the Hamiltonian form and approximation level. The time-dependent density functional method (TDDFT Hamiltonian form) was applied to compute electronic excitation energies, and the correct order of excitation states was given for a macrocycle compound of porphin.[22] Here, the calculation of γ is concerned only with the transition moments (i.e., state functions) and energy from the SOS method,[29] and the TDDFT method is selected to compute the state functions and energies in this work. It should not be surprising that calculations of γ are sensitive to the treatment of electron−electron interactions (EEI). In the context of the ab initio HF model, the treatment of EEI via configuration interaction must include at least single- and double-excitation configuration interaction to yield correct γ values.[28] However, configuration interaction is included in a natural way in the TDDFT calculations.[30] Accordingly, a time-dependent DFT formalism is employed to compute frequency-dependent response functions of γ, and it will rectify the EEI problems of the ab initio SCF approximation at comparable or even lower computational cost.[22]

3. Results and Discussions

3.1. Geometrical Structures. The optimized geometries are shown in Figure 1, which also shows the numbering scheme of atoms. Some calculated bond lengths and angles of the MPcCl (M = Al, Ga, In) molecules are listed in Table 1 at the RHF/6-31G* and RHF/3-21G levels, respectively. In Figure 1, the

TABLE 1: Calculated Bond Lengths and Bond Angles and Corresponding Experimental Values

Bond Lengths (Å)							
		AlPcCl			GaPcCl		InPcCl
bond	3-21G	6-31G*	exptl	3-21G	6-31G*	exptl	3-21G
M−Cl	2.275	2.178	2.179	2.308	2.210	2.217	2.455
M−N1	1.971	1.995	1.961	1.991	2.022	1.979	2.132
M−N2	1.970	1.982	1.962	1.988	2.009	1.981	2.121
M−N3	1.962	1.956	1.966	1.975	1.981	1.983	2.132
M−N4	1.970	1.982	2.018	1.988	2.009	1.988	2.135
Bond Angles (deg)							
		AlPcCl			GaPcCl		InPcCl
angle	3-21G	6-31G*	exptl	3-21G	6-31G*	exptl	3-21G
Cl−M−N1	100.0387	101.995	102.74	101.4795	102.635	103.11	108.1776
Cl−M−N2	100.9701	103.485	100.74	102.812	104.343	102.81	110.9495
Cl−M−N3	102.425	105.865	102.44	104.7427	107.071	102.41	108.193
Cl−M−N4	100.9883	103.483	102.14	102.8564	104.343	102.91	106.0027
N1−M−N2	87.1947	85.601	86.85	86.3058	85.103	87.32	85.1811
N1−M−N4	87.1905	85.599	88.05	86.3098	85.104	87.32	83.4307
N2−M−N3	88.55	87.940	84.95	87.8992	87.582	87.12	85.179
N3−M−N4	88.5473	87.939	90.45	87.9052	87.582	87.02	83.4305

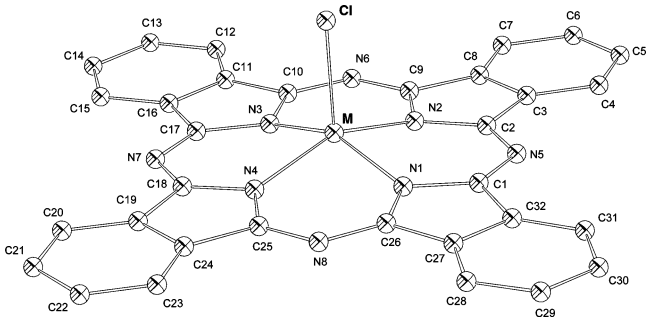

Figure 1. MPcCl molecular configuration (M = Al, Ga, In).

N atoms numbered from 1 to 4 are called the isoindole nitrogens, and these nitrogen atoms make a plane. The Cl atom is the axial ligand of the macrocycle. The central metal atom M situated at the N4 plane has a coordinate number of 5. The calculated distances between M and the N4 plane are 0.379, 0.446, and 0.653 Å, respectively, and the calculated M−Cl bond lengths increase from 2.275 to 2.308 to 2.455 Å on going down from Al to In atoms in the periodic table for the MPcCl (M = Al, Ga, In) molecules when using a basis set at the 3-21G level. The calculated distances at the RHF/6-31G* level between M (M = Al, Ga) and the N4 plane are separately 0.470 and 0.507 Å, and the M−Cl (M = Al, Ga) bond lengths are 2.179 and 2.210 Å, respectively. The calculated M−N (M = Al, Ga, In) bond lengths lie in the ranges of 1.962−1.971, 1.975−1.991, and 2.121−2.135 Å, respectively. The calculated C−N bond lengths lie in the range of 1.276−1.410 Å, the C−C distances lie in the range of 1.365−1.475 Å, and the C−H bond length is 1.071 Å. The calculated lengths of the C−N, C−C, and C−H bonds display no significant differences among the three MPcCl molecules. The calculated average N−N distances at the RHF/3-21G level among the isoindole nitrogens are 2.731, 2.736, and 2.858 Å, respectively. Comparing the N−N distances among the MPcCl (M = Al, Ga, In), we find that the size of the inner cavity of the phthalocyanine macrocycle has a small variation. A central ion M crowds out the cavity and is situated about the N4 plane. This space arrangement will be favorable in energy. Accordingly, the larger the M ion is, the greater the distance between the M and N4 plane becomes in MPcCl (M = Al, Ga, In). The calculated bond angles Cl−M−N lie in the ranges of 100.04−102.43°, 101.48−104.74°, and 106.00−110.95°, and the calculated bond angles N−M−N between the neighboring N atoms are in the ranges of 87.19−88.55°, 86.31−87.90°, and 83.43−85.18°, respectively, in the MPcCl molecules (M = Al, Ga, In). We show that the calculated molecular structures of MPcCl have distorted C_{4v} symmetry. The calculated M−Cl bond at the RHF/3-21G level is away from the C_4 axis of the undistorted square N4 plane to be about from 10 to 20° for MPcCl (M = Al, Ga, In) molecules. The further the metal is coordinated away from the N4 plane, the greater the isoindole units have to rotate and the more distorted the molecule becomes. This situation is due to the fact that the M ion radii increase in the order of Al < Ga < In in the MPcCl molecules.

Table 1 also gives a comparison between HF/3-21G and HF/6-31G* as well as experimental bond lengths in the MPcCl (M = Al, Ga) molecules. Experimental N−C distances from X-ray crystallographic investigations lie in the ranges of 1.28−1.53 and 1.309−1.386 Å, and experimental M−Cl distances are 2.179 and 2.217 Å; averages M−N distances are 1.977 and 1.983 Å for the MPcCl (M = Al, Ga) crystals,[31] respectively. The correlation here between theoretical and experimental lengths is very good, as shown in Table 1. The calculated M−Cl length at the 3-21G basis set level is an overestimation of about 0.090 Å, and the average error is 0.002 Å for the M−N bond in the MPcCl (M = Al, Ga) molecules. Our calculated M−Cl (M = Al, Ga) lengths at the 6-31G* basis set level are very close to the experimental values. Here, we note that the experimental and calculated geometries at the 6-31G* level are not available for the InPcCl molecule. In the following text, we consider only systematic comparisons and variation trends in excited-state properties and dynamic third-order polarizabilities among the MPcCl (M = Al, Ga, In) molecules. Accordingly, the optimized geometries at 3-21 basis sets will be employed to calculate the physical properties.

3.2. Excited-State Properties. The transition energies, moments, and oscillator strengths of 60 excited states from the optimized geometries are calculated at the TDDFT B3LYP/3-21G* level for the MPcCl (M = Al, Ga, In) molecules. Table 2 lists the transition electric dipole moments from the ground state to some important excited states. It is found that the electric dipole transition is allowable in the *x* and *y* directions and forbidden in the *z* direction; that is, the moments in the axis direction (*z*) are almost zero. These calculated results describe the behavior of charge transfer in molecules with a 2D structure. Figures 2 give the relationships between the oscillator strengths

TABLE 2: Calculated Transition Energies, Moments, and Oscillator Strengths of Some Excited States

state	energy (eV)	moment (au) *x*	*y*	*z*	oscillator strength
		AlPcCl			
S1	2.1790	0.0098	2.4291	−0.0006	0.0252
S2	2.2053	−2.3890	0.0102	0.0000	0.0250
S3	3.0251	0.2419	0.0006	0.0003	0.0005
S17	3.7311	−0.0242	0.2508	−0.0189	0.0008
S18	3.7378	0.6111	0.0020	−0.0019	0.0047
S25	3.8387	−2.3727	0.1208	−0.0008	0.0749
S26	3.8405	0.1370	2.0155	−0.0187	0.0542
		GaPcCl			
S1	2.1779	−0.0025	−2.4125	0.0025	0.0249
S2	2.2056	2.3705	−0.0025	0.0000	0.0246
S3	3.1293	0.2525	−0.0021	−0.0001	0.0006
S17	3.7314	−0.0112	−0.3046	−0.0159	0.0012
S18	3.7397	0.0052	−0.6168	−0.1711	0.0052
S25	3.8417	−2.2274	0.2070	−0.0047	0.0665
S26	3.8422	0.3064	1.6329	−0.0370	0.0367
		InPcCl			
S1	2.1010	0.0008	2.3737	−0.0068	0.0224
S2	2.1357	−2.3118	0.0009	−0.0001	0.0219
S6	3.4255	−0.0505	0.6922	−0.0600	0.0051
S12	3.6138	0.0081	−0.1123	0.0808	0.0002
S14	3.6402	−0.0091	−1.3234	0.1596	0.0212
S22	3.7731	1.6078	−0.0193	−0.0041	0.0331
S24	3.8103	−0.0011	1.3042	−0.0654	0.0223

and absorption wavelengths for the lowest 30 excited states. It is found that the MPcCl (M = Al, Ga, In) exhibit electronic transitions in the visible at about 600 nm (Q band) and in the near-UV from 300−400 nm (B band). The Q band is sharp and arises almost exclusively from transitions of $\pi-\pi^*$ states. For example, the first excited state S_1 is mostly due to contributions from the configurations of 0.5504($MO_{147} \rightarrow MO_{148}$), 0.5525-($MO_{156} \rightarrow MO_{157}$), and 0.5520($MO_{165} \rightarrow MO_{166}$) for the MPcCl (M = Al, Ga, In), respectively. The HOMO (MO_{147} for AlPcCl, MO_{156} for GaPcCl, and MO_{165} for InPcCl) is exclusively formed from the C p_z orbitals, and the LUMO (MO_{148} for AlPcCl, MO_{157} for GaPcCl, and MO_{166} for InPcCl) is formed from C p_z orbitals mixing with N p_z orbitals for the three title molecules. We take the HOMO and LUMO of InPcCl as examples and plot them in Figure 3. It is found that the electronic charge is well distributed and that the Q band is mostly localized on the Pc ring. However, in comparing the first transition wavelengths among the MPcCl (M = Al, Ga, In) molecules, we find that there is no change between AlPcCl and GaPcCl and that there is a red shift from 570 (569) to 590 nm for AlPcCl (GaPcCl) to InPcCl. Why is this the case? The calculated gross orbital populations show that there are 10.0 d electrons in the Ga atom and 19.8 d electrons in the In atom. Accordingly, we can say that the valence electronic structures are almost the same, resulting in no shift of the first transition wavelength between the AlPcCl and GaPcCl molecules, and that the valence d-electrons to Pc-ring charge transfer induces a red shift of the first transition wavelength in the InPcCl molecule.

The B band, as shown in Figure 2, is broad, and the band has a blue shift from Al to In for the MPcCl (M = Al, Ga, In) molecules. For example, the transition wavelengths of the S_3 states are 410, 396, and 381 nm for the MPcCl (M = Al, Ga, In), respectively. The reason for this shift can be explained from the largest configuration components contributing to the excited state of S_3: 0.6891($MO_{146} \rightarrow MO_{148}$), 0.6819($MO_{155} \rightarrow MO_{157}$), and 0.5113($MO_{164} \rightarrow MO_{166}$) for the MPcCl (M = Al, Ga, In) molecules. The HOMO-1 orbital (MO_{146} for AlPcCl, MO_{155} for GaPcCl, and MO_{164} for InPcCl) mixes with σ-orbital character

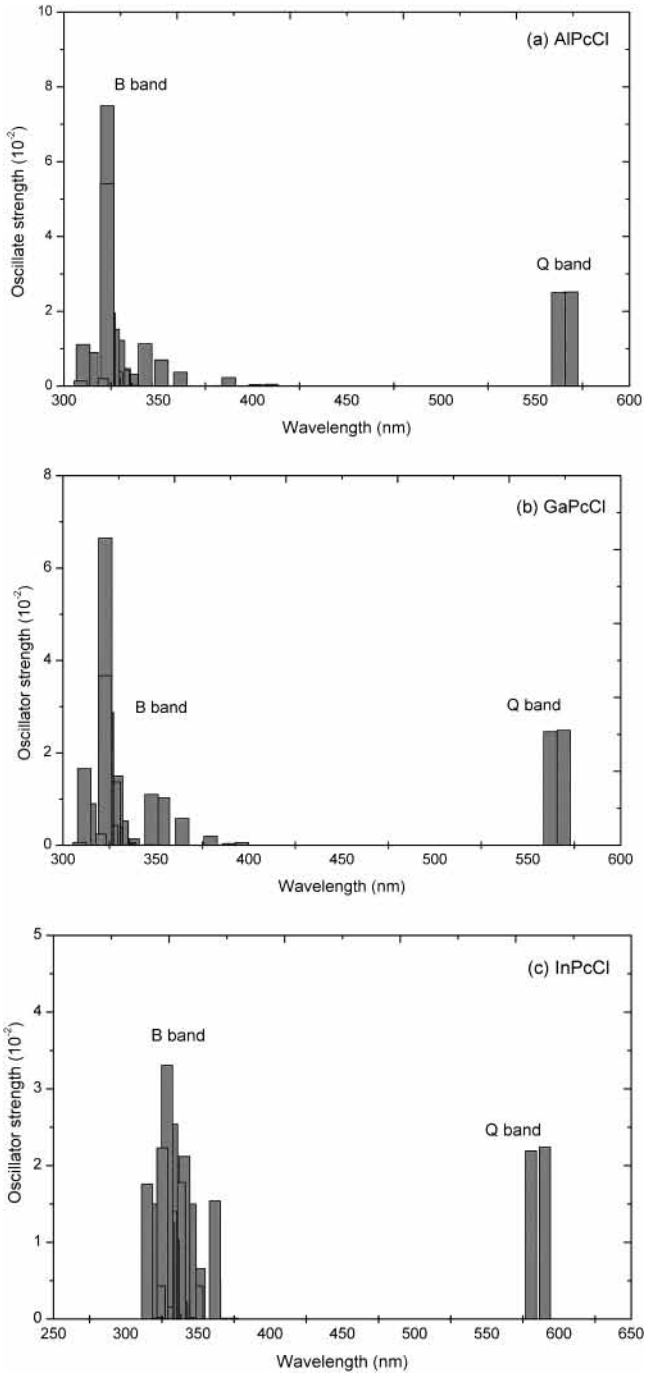

Figure 2. Calculated absorption spectrum at the TDDFT B3LYP/3-21G* level for MPcCl (M = Al, Ga, In).

increasing from AlPcCl to InPcCl, and the Cl p orbital in turn decreases from the MPcCl (M = Al, Ga, In) molecules, as shown in Figure 4. Accordingly, the blue shifts of the B band depend on the strength of the $\sigma-\pi$ interactions in the MPcCl (M = Al, Ga, In) molecules. It is found from Figure 2 that the our calculated Q and B bands match the experimental results of the Q band from 600−700 nm and the B band from 300−400 nm in the GaPcCl and PcAlF molecules.[8]

3.3. Dynamic Third-Order Polarizabilities. The transition energies from the ground state to 60 excited states, the electronic dipole moments of the ground state and 60 excited states, and the transition moments from the ground state to excited states and between excited states are calculated by the TDDFT method based on the B3LYP/3-21G* level. These values obtained from the TDB3LYP calculations are taken as input for the SOS

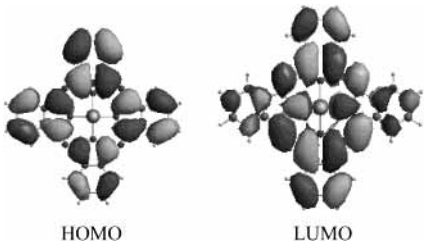

Figure 3. Frontier orbitals of InPcCl.

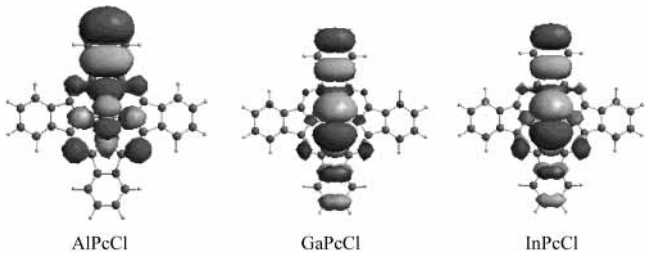

Figure 4. HOMO-1 orbital of MPcCl (M = Al, Ga, In).

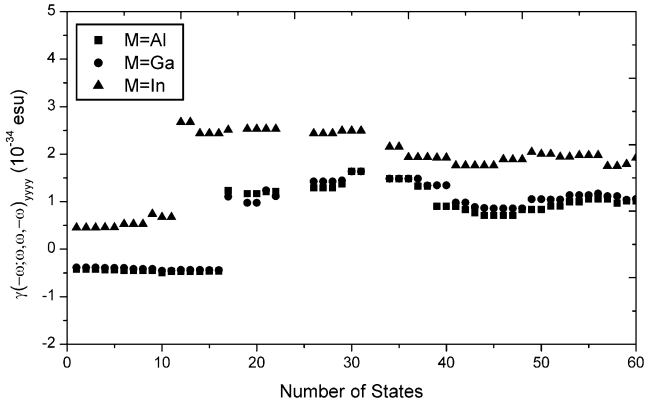

Figure 5. Convergence behavior of γ with the number of states considered in the SOS calculations at TDF B3LYP/-321G* for MPcCl (M = Al, Ga, In).

equation. For the calculations of γ, we first consider how to truncate the infinite SOS expansion to a finite one. Figure 5 shows the plots of the calculated third-order polarizabilities for the DFWM optical process, γ_{yyyy} having the largest component, versus the number of states for the MPcCl (M = Al, Ga, In) molecules for the static case ($\hbar\omega = 0.0$ eV). It is found that the three curves have a similar shape, that is, similar convergence behavior to that of γ_{yyyy} in the MPcCl molecules. The segments of the curves formed below state 17 for AlPcCl and GaPcCl and below state 12 for InPcCl are smooth. The calculated values of γ_{yyyy} including 16 states are about 45 and 42% of the γ_{yyyy} value including 60 states for AlPcCl and GaPcCl and about 35% of that for InPcCl. The segments of the curves formed from state 17 for AlPcCl and GaPcCl or from state 13 for InPcCl to state 40 oscillate, and the segments of the curves formed after state 41 are again smooth. The calculated γ_{yyyy} values obtained from the summation over 20 states from the 41th state to the 60th state are about 11, 7, and 8% of the γ_{yyyy} value obtained from the summation over 60 states for the MPcCl (M = Al, Ga, In), respectively, using the SOS method. This is reasonable in calculations of γ for MPcCl (M = Al, Ga, In) molecules when we truncate 60 states in a summation over states.

Figure 6 depicts the dynamic γ_{yyyy} with different optical physical processes from frequency 0.0 to 1.8 eV/$\hbar$ for the ground state in MPcCl (M = Al, Ga, In) molecules. For the static case where the input photon energy is zero, the values of all three processes THG, EFISHG, and DFWM have the same number for each molecule, and they are in the order of AlPcCl (1.017×10^{-34}) < GaPcCl (1.056×10^{-34}) < InPcCl (1.925×10^{-34} esu). Figure 6 also shows a correlation between the dispersion curve of γ_{yyyy} and the absorption spectrum of the Q-band region. Note that different dispersion behavior takes place in different optical processes. The first resonant appearance in the dispersion curve requires an energy difference of zero between the transition energy and 3 times the input photon energy ($E_{trans} - 3\hbar\omega = 0$) in the THG process; $E_{trans} - 2\hbar\omega = 0$ in the EFISHG and DFWM processes. Figure 6 shows evidence of this in that the first near-resonant enhancement appears at about $\hbar\omega = 0.60$ eV for the THG process and at about $\hbar\omega = 0.90$ eV for the EFISHG or DFWM process. Accordingly, from the dispersion curve we can make a crude determination of the absorption region of the Q band localized at about 14 520 cm^{-1} (3×0.60 or 2×0.90 eV) for the MPcCl (M = Al, Ga, In). This estimated value is close to the observed value of about 14 000 cm^{-1} (700 nm) for PcAlF and GaPcCl in solution.[9] Therefore, we can choose an input wavelength to obtain the nonresonant third-order polarizability among the measuring techniques of the THG, EFISHG, and DFWM processes from a known transition energy or absorption spectrum of a given material. It is also found from Figure 6 that $\gamma(\omega)_{yyyy}$ in the DFWM process has a wide nonresonance frequency region and shows pronounced resonance at magnitudes of 5.300×10^{-34}, 5.453×10^{-34}, and 17.453×10^{-34} esu for the MPcCl (M = Al, Ga, In), respectively. Away from resonance, at 0.650 eV, the $\gamma(\omega)_{yyyy}$ values of the MPcCl (M = Al, Ga, In) are 1.677×10^{-34}, 1.729×10^{-34}, and 3.340×10^{-34} esu. By comparing the MPcCl (M = Al, Ga, In) molecules, as plotted in Figure 7, we find that the calculated third-order polarizabilities γ increase in the order of AlPcCl ≤ GaPcCl < InPcCl. The reasons that InPcCl has the largest third-order polarizability are that the largest ion radius M and the loose d electrons of the In atom participate in electronic charge transfer. The metal In to Pc-ring charge-transfer states are the lowest in energy among the MPcCl (M = Al, Ga, In) molecules, as seen in Table 2. The lower the transition energy, the larger the third-order polarizability according to the SOS method.

3.4. Comparison to Experiments. In this section, we will compare our predictions with the measured results of third-order optical susceptibilities for MPcCl (M = Al, Ga, In). The third-order nonlinear optical susceptibility of a film can be thought of as being built up from the corresponding susceptibility of individual molecules, and the film susceptibility has a relationship to the polarizability of a molecule. Therefore, the third-order nonlinear susceptibility of the film can be calculated using the second-order hypolarizability of molecule, the local-field correction factor, and the molecular number density. In this way, the third-order nonlinear optical susceptibility of an MPcCl film is defined as

$$\chi^{(3)} = NF\langle\gamma\rangle \tag{2}$$

where N is the molecular density number and F is the local field factor that depends on the radiation frequency. We note here that the molecular number density, N, is defined as the product of the mass density, D, and Avogadro's constant, L, divided by the molar mass, M. For AlPcCl, using $M = 579.00$ g mol^{-1} and $D = 1.54$ g cm^{-3},[31] we obtained $N = 1.602 \times 10^{21}$ cm^{-3}. With the assumption of a Lorentz−Lorenz local field,[32] $f_\omega = [n_\omega^2 + 2]/3 = 1/[1 - (4\pi/3)N\alpha_\omega]$. Accordingly, the local field factor f_ω can be obtained by the refractive index or the first-order microscopic polarizability and described as the

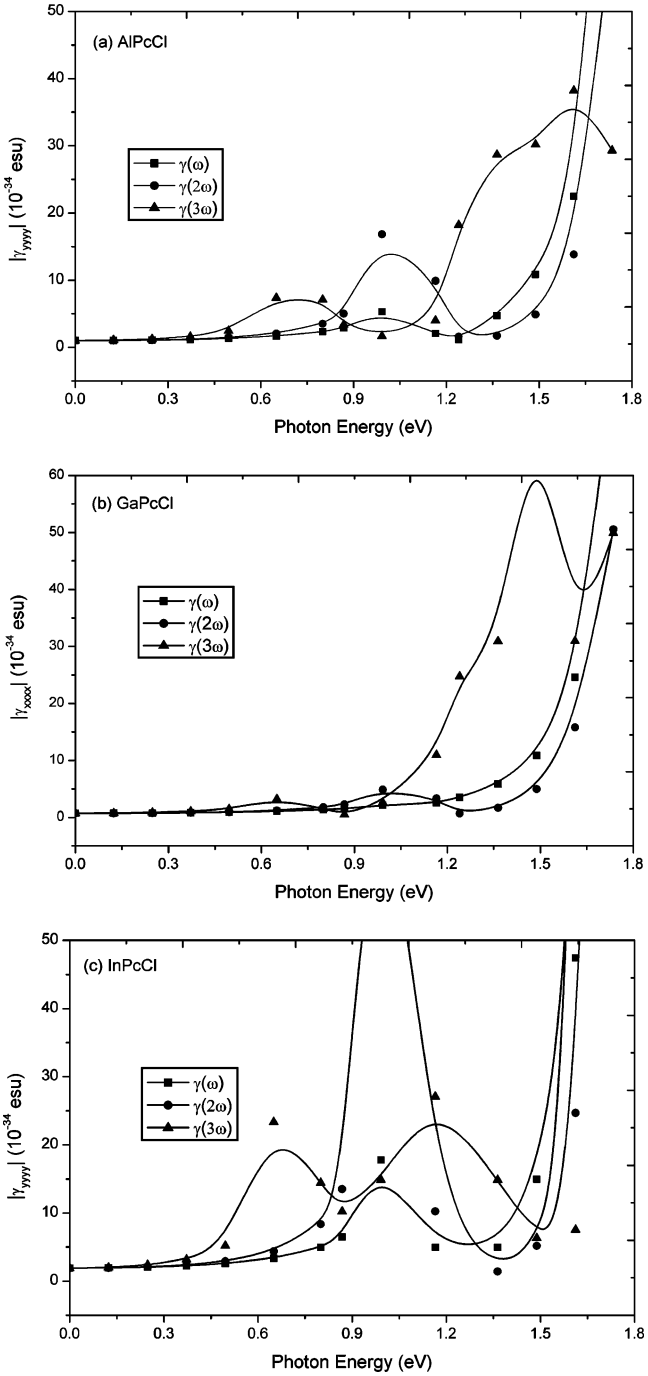

Figure 6. Dynamic third-order optical polarizabilities of three optical processes at the SOS//B3LYP/3-21*//RHF/3-21G level for MPcCl (M = Al, Ga, In).

interaction between a selected molecule and the surrounding molecules in the film.[33] Table 3 lists the calculated number density N and local-field correction factor F, which is equal to (f_ω).[4] The average value $\langle\gamma\rangle$ is set equal to γ_{yyyy} because of the fact that the γ components of MPcCl (M = Al, Ga, In) have good symmetry in the xy plane and are almost zero for the axis direction in the nonresonant frequency zone. The calculated values $\chi^{(3)}$ of MPcCl (M = Al, Ga, In) films are listed in Table 3 for the DFWM optical process at an input wavelength of 1905 nm. The measured values $\chi^{(3)}$ of MPcCl films are also listed in Table 3 for the THG optical process at an input wavelength of 1064 nm for M = Ga and 1097 nm for M = Al, In. Although it is shown that the experiment values of $\chi^{(3)}(-3\omega; \omega, \omega, \omega)$ are 2 to 6 times the calculated values of $\chi^{(3)}(-\omega; \omega, \omega, -\omega)$

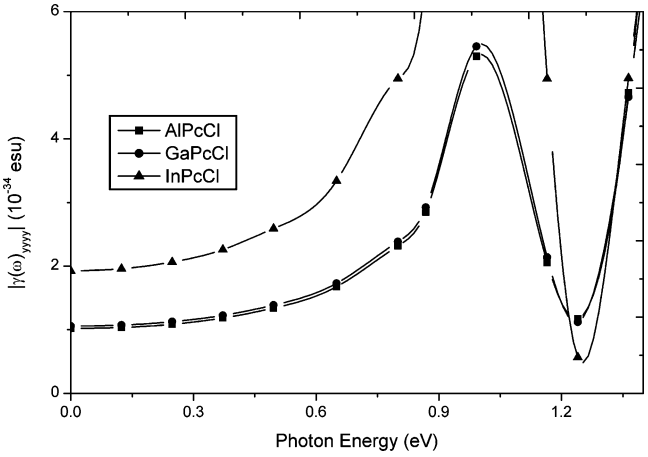

Figure 7. Third-order polarizabilities of the DFWM process at the SOS//B3LYP/3-21G*//RHF/3-21G level for MPcCl (M = Al, Ga, In).

TABLE 3: Parameters for Calculating the NLO Susceptibilities of MPcCl Films at 1905 nm for the DFWM Optical Process

form		N^a	F	$\langle\gamma\rangle^b$	$\chi^{(3)}$ (calcd)^c	$\chi^{(3)}$ (exptl)^c
M =	Al	1.602	5.256	5.031	0.424	1.5[13]
	Ga	1.599	5.009	5.187	0.415	2.5[6]
	In	1.570	4.926	10.019	0.775	13.0[13]

^{a} 10^{21}/cm^3. ^{b} 10^{-34} esu. ^{c} 10^{-11} esu.

among the comparisons of MPcCl (M = Al, Ga, In) films, both the experimental and theoretical results show the increasing trend of third-order susceptibility $\chi^{(3)}$ in the order of AlPcCl < GaPcCl < InPcCl. This means that the value of $\chi^{(3)}$ increases as the M ion radius and that the d-electron charge transfer increases in the same column in the periodic table for MPcCl.

4. Conclusions

The optimized structures show that the MPcCl molecules have distorted C_{4v} symmetry and that the larger the M ion radius is, the further the M metal is coordinated away from the N4 plane and the more distorted the molecule becomes among the MPcCl (M = Al, Ga, In) molecules. The calculated bond lengths and bond angles are compared with the X-ray-determined crystal structural data except that the data of InPcCl has not been obtained in the experiments. The calculated properties of excited states show that valence d-electrons to Pc-ring charge transfer induces a red shift of the Q band in the InPcCl molecule. The calculated dynamic third-order polarizabilities of the all three processes THG, EFISHG, and DFWM show varied trends in the order of AlPcCl < GaPcCl < InPcCl at a nonresonant frequency. We also found correlations between the dispersion behavior of γ and the absorption spectra of Q-band regions, which verifies that the first resonance enhancement of third-order polarizability should appear at one-third or one-half of the transition energy for the THG or DFWM process in the ground state for a given material. The calculated susceptibilities of $\chi(-\omega; \omega, \omega, -\omega)$ of MPcCl films are in agreement with the available measuring values in order of magnitude at an input wavelength of 1907 or 1064 nm. Both the theoretical and experimental results for third-order NLO susceptibilities show an increase in the order of AlPcCl < GaPcCl < InPcCl. The largest third-order NLO response of the InPcCl film arises from the largest distortion away from C_{4v} symmetry and the largest d-electron to Pc-ring charge transfer among MPcCl (M = Al, Ga, In) materials.

Acknowledgment. This investigation was supported by the National Science Foundation of China (no. 90201015), the Science Foundation of the Fujian Province (nos. E0210028 and 2002F010), and the Foundation of State Key Laboratory of Structural Chemistry (no. 030060).

References and Notes

(1) Mckeown, N. B. *Phthalocyanine Materials: Synthesis, Structure and Function*; Cambridge University Press: Cambridge, England, 1998.

(2) Somani, P. R.; Radhakrishnan, S. *Mater. Chem. Phys.* **2003**, *77*, 117.

(3) *Phthalocyanine Properties and Applications*; Leznoff, C. C., Lever, A. B. P., Ed; VCH Publishers: Cambridge, England, 1989, 1993, and 1996; Vols. 1−4,

(4) Jain, S. L.; Sain, B. *J. Mol. Catal. A: Chem.* **2003**, *195*, 283.

(5) Fernandez-Alonso, F.; Marovino, P.; Paoletti, A. M.; Righini, M.; Rossi, G. *Chem. Phys. Lett.* **2002**, *356*, 607.

(6) Manas, E. S.; Spano, F. C.; Chen, L. X. *J. Chem. Phys*. **1997**, *107*, 707.

(7) Terasaki, A.; Hosoda, M.; Wada, T.; Tada, H.; Koma, A.; Yamada, A.; Sasabe, H.; Garito, A. F.; Kobayashi, T. *J. Phys. Chem*. **1992**, *96*, 10534.

(8) Nakano, H.; Okumura, N.; Maeda, A.; Furuhashi, H.; Yoshikawa, T.; Uchida, Y.; Kojima, K.; Ohashi, A.; Ochiai, S.; Mizutani, T. *Ieice. T. Electron*. **2000**, *E83C*, 1114.

(9) Ho, Z. Z.; Ju, C. Y.; Hetherington, W. M., III. *J. Appl. Phys*. **1987**, *62*, 716.

(10) Nalwa, H. S.; Saito, T.; Yamada, A.; Iwayanagi, T. *J. Phys. Chem*. **1993**, *97*, 10515.

(11) Shirk, J. S.; Lindle, J. R.; Bartoli, F. J.; Boyle, M. E. *J. Phys. Chem*. **1992**, *96*, 5847.

(12) Diaz-Garcia, M. A.; Agullo-Lopez, F.; Torruellas, W. E.; Stegeman, G. I. *Chem. Phys. Lett*. **1995**, *235*, 535.

(13) Sakai, Y.; Ueda, M.; Yahagi, A.; Tanno, N. *Polymer* **2002**, *43*, 3497.

(14) Diaz-Garcia, M. A.; Ledoux, I.; Duro, J. A.; Torres, T.; Agullo-Lopez, F.; Zyss, J. *J. Phys. Chem*. **1994**, *98*, 8761.

(15) Kanbara, H.; Maruno, T.; Yamashita, A.; Matsumoto, S.; Hayashi, T.; Konami, H.; Tanaka, N. *J. Appl. Phys*. **1996**, *80*, 3674.

(16) Shirk, J. S.; Lindle, J. R.; Bartoli, F. J.; Hoffman, C. A.; Kafafi, Z. H.; Snow, A. W. *Appl. Phys. Lett*. **1989**, *55*, 1287.

(17) Matsuda, H.; Okada, S.; Masaki, A.; Nakanishi, H.; Suda, Y.; Shigehara, K.; Yamada, A. *SPIE Proc*. **1990**, *1337*, 105.

(18) Nalwa, H. S.; Hanack, M.; Pawlowski, G.; Engel, M. K. *Chem. Phys*. **1999**, *245*, 17.

(19) Hanack, M.; Schneider, T.; Barthel, M.; Shirk, J. S.; Flom, S. R.; Pong, R. G. S. *Coord. Chem. Rev*., **2001**, *219*, 235.

(20) Frisch, M. J.; Trucks, G. W.; Schlegel, H. B.; Scuseria, G. E.; Robb, M. A.; Cheeseman, J. R.; Zakrzewski, V. G.; Montgomery, J. A., Jr.; Stratmann, R. E.; Burant, J. C.; Dapprich, S.; Millam, J. M.; Daniels, A. D.; Kudin, K. N.; Strain, M. C.; Farkas, O.; Tomasi, J.; Barone, V.; Cossi, M.; Cammi, R.; Mennucci, B.; Pomelli, C.; Adamo, C.; Clifford, S.; Ochterski, J.; Petersson, G. A.; Ayala, P. Y.; Cui, Q.; Morokuma, K.; Malick, D. K.; Rabuck, A. D.; Raghavachari, K.; Foresman, J. B.; Cioslowski, J.; Ortiz, J. V.; Stefanov, B. B.; Liu, G.; Liashenko, A.; Piskorz, P.; Komaromi, I.; Gomperts, R.; Martin, R. L.; Fox, D. J.; Keith, T.; Al-Laham, M. A.; Peng, C. Y.; Nanayakkara, A.; Gonzalez, C.; Challacombe, M.; Gill, P. M. W.; Johnson, B. G.; Chen, W.; Wong, M. W.; Andres, J. L.; Head-Gordon, M.; Replogle, E. S.; Pople, J. A. *Gaussian 98*, revision A.9; Gaussian, Inc.: Pittsburgh, PA, 1998.

(21) Casida, M. E.; Jamorski, C.; Casida, K. C.; Salahub, D. R. *J. Chem. Phys*. **1988**, *180*, 4439.

(22) Bauernschmitt, R.; Ahlrichs, R. *Chem. Phys. Lett*. **1996**, *256*, 454.

(23) Stratman, R. E.; Scuseria, G. E.; Frisch, M. J. *J. Chem Phys*. **1998**, *109*, 8218−8224.

(24) Gross, E. K. U.; Kohn, W. *Adv. Quantum Chem*. **1990**, *21*, 255.

(25) Runge, E.; Gross, E. K. U. *Phys. Rev. Lett*. **1984**, *52*, 977.

(26) Ward, J. F. *Rev. Mod. Phys*. **1965**, *37*, 1.

(27) Orr, B. J.; Ward, J. F. *Mod. Phys*. **1971**, *20*, 513.

(28) Pierce, B. M. *J. Chem. Phys*. **1989**, *91*, 791.

(29) Andre, J.-M.; Barbier, C.; Bodart, V.; Delhalle, J. In *Nonlinear Optical Properties of Organic Molecules and Crystals*; Chemla, D. S., Zyss, J., Eds.; Academic Press: New York, 1987; Vol. 2, pp 137.

(30) van Gisbergen, S. J. A.; Snijders, J. G.; Baerends, E. J. *Comput. Phys. Commun.* **1999**, *118*, 119.

(31) Wynne, K. J. *Inorg. Chem*. **1984**, *23*, 4658.

(32) Boyd, R. W. *Nonlinear Optics*; Academic Press: San Diego, CA, 1992; p 148.

(33) Cheng, W.-D.; Zhang, H.; Lin, Q.-S.; Zheng, F.-K.; Chen, J.-T. *Chem. Mater*. **2001**, *13*, 1841.